J Mar Sci Technol (2014) 19:15–32
DOI 10.1007/s00773-013-0229-y

ORIGINAL ARTICLE

An insight into the slamming behaviour of large high-speed catamarans through full-scale measurements

Gunnar Jacobi · Giles Thomas · Michael R. Davis · Gary Davidson

Received: 5 September 2012 / Accepted: 5 July 2013 / Published online: 24 July 2013

Abstract The slamming behaviour of a large high-speed catamaran has been investigated through the analysis of full-scale trials data. The US Navy conducted the trials in the North Sea and North Atlantic region on a 98 m wave piercer catamaran, *HSV-2 Swift*, designed by Revolution Design Pty Ltd and built by Incat Tasmania. For varying wave headings, vessel speeds and sea states the data records were interrogated to identify slam events. An automatic slam identification algorithm was developed, considering the measured rate of change of stress in the ship's structure coupled with the vessel's pitch motion. This has allowed the slam occurrence rates to be found for a range of conditions and the influence of vessel speed, wave environment and heading to be determined. The slam events have been further characterised by assessing the relative vertical velocity at impact between the vessel and the wave. Since the ship was equipped with a ride control system, its influence on the slam occurrence rates has also been assessed.

Keywords Slamming · High-speed catamaran · Full-scale measurements · Ride control system · Ship motions

G. Jacobi is a visiting researcher from University of Rostock, Germany.

G. Jacobi · G. Thomas (✉)
Australian Maritime College, University of Tasmania,
Locked Bag 1395, Launceston, TAS 7250, Australia
e-mail: giles@amc.edu.au

M. R. Davis
University of Tasmania, Hobart, TAS, Australia

G. Davidson
Revolution Design Pty Ltd, Derwent Park, TAS, Australia

1 Introduction

Large high-speed catamarans are currently used for both commercial and military operations. They have seen a rapid development over the last 20 years, with the largest craft built in 1992 being 73 m [1], whilst in 2012, Incat Tasmania produced vessels of 112 m in length and Austal Ships in Western Australia delivered a catamaran ferry of 113 m. These vessels are designed with an emphasis on minimising structural weight to enable the ratio of deadweight to lightship to be maximised, and thus to achieve a high vessel speed, whilst maintaining structural integrity in severe ocean environments. In the past, this conflict of requirements has led to problems, and several large high-speed catamarans are known to have suffered damage in extreme sea conditions, although details on such incidents are usually difficult to obtain due to the desire of shipbuilders and operators to minimise publicity of such events; exceptions include Rothe et al. [2] and Thomas et al. [3]. Therefore, it is crucial that designers are provided with accurate wave loading information to determine appropriate design load cases for structural analyses in the design process.

The wave loads experienced by large high-speed catamarans can be split into two main categories: global wave loads and impact loads. Previous work has shown [3] that it is the impact loads, such as slamming, that dominate the creation of large bending moments in the vessels when operating in waves. After a slam event, the vessel may experience whipping as the natural modes of the structure are excited; in particular, the first longitudinal mode of vibration [4]. This whipping may make a significant contribution to reducing the fatigue life of a vessel [5].

For conventional slow-speed monohulls, classification societies have used an empirical approach based on operational experience to determine design rules, and these rules are formulated using parametric relationships to determine design loads. With the rapid development of high-speed craft classification societies, there has been a lack of operational data on which to base the structural rules, so in addition to the empirically-based rules, classification societies have introduced direct calculation methods.

To supplement this work by classification societies, it is critical that full-scale measurements are obtained to determine the magnitude of wave loads on vessels in varying conditions and determine their influences. However, since trials are expensive to conduct and usually confidential to the ship builder or owner, results for high-speed multihulls are very limited in the published literature. Exceptions include the work of Steinmann et al. [6] on an 86 m catamaran built by Austal Ships, and the measurement programmes on a series of Incat vessels (81, 86, 96 and 98 m) by Roberts et al. [7], Thomas et al. [8], and Amin et al. [9]. In addition, Fu et al. [10] report on an Office of Naval Research (ONR)-sponsored project to obtain full-scale qualitative and quantitative wave slamming and ship motion data on the X-craft, an 80 m high-speed catamaran.

The results presented in this paper arise from full-scale trials completed on *HSV-2 Swift*, a 98 m Incat catamaran, while operating in coastal waters off Norway and off the north-west coast of the United Kingdom in the North Atlantic. For varying wave headings, vessel speeds and sea states the data records were interrogated to identify slam events. This has allowed the slam occurrence rates to be found for a range of conditions, and the influence of vessel speed, wave environment and heading to be determined. The slam events have been further characterised by assessing the relative vertical velocity at impact between the vessel and the wave. Since the ship was equipped with a ride control system, its influence on the slam occurrence rates has also been assessed, providing insight into the possible use of such systems to reduce the structural loads on high-speed catamarans.

2 Full-scale trials

2.1 Vessel details

HSV-2 Swift (Hull 61), shown in Fig. 1, is a 98 m wave-piercer catamaran, designed by Revolution Design and built by Incat Tasmania. *HSV-2 Swift* is an aluminium catamaran powered by four diesel engines and using a water jet propulsion system. It has a maximum operational speed of 38 knots and can achieve 42 knots in the lightship configuration.

From a structural perspective, in cross section the vessel is essentially a dual box-like structure: the outer box incorporates the demihulls through to portals and horizontal cross bracing, whilst the inner box consists of the deck, vertical cross bracing and longitudinal inboard structure, as shown in Fig. 2. The majority of the longitudinal strength is gained from the aluminium longitudinal

Fig. 1 Incat Hull 61 *HSV-2 Swift*

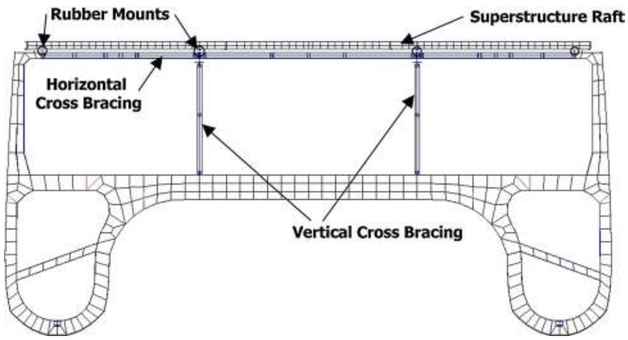

Fig. 2 Cross section of hull girder showing *dual box*-like structure

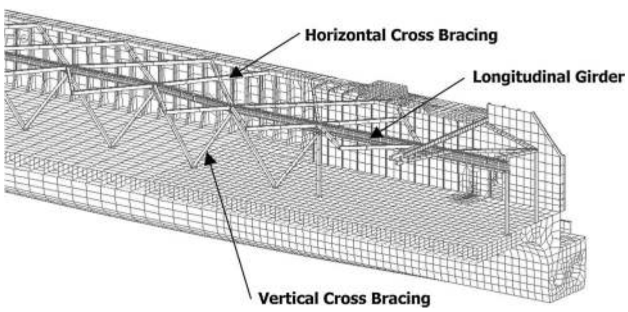

Fig. 3 Cut away section of hull girder (starboard side) showing *horizontal* and *vertical cross bracing*

girders and vertical steel cross bracing. Steel is used for the vertical cross bracing to keep structural member dimensions to a minimum, thus maximizing available vehicle deck space. The horizontal cross bracing, for which aluminium extrusions are used, takes the majority of the torsional and transverse loads, as shown in Fig. 3. Since the aft end of the vehicle deck is open for loading and unloading of vehicles, an opportunity is lost for additional strength in torsion. Therefore, the aft bulkhead uses thick plate (~40 mm) in order to absorb the load. The vessel's superstructure, which accommodates all the passenger areas and operating bridge, is resiliently mounted onto the main hull girder using rubber mounts, with the aim of reducing noise and vibration within the superstructure.

Similar to all Incat vessels, *HSV-2 Swift* has a distinct centrebow between the two demi-hulls at the front of the vessel, as shown in Fig. 4. This is designed to counter deck diving in following seas, and reduce vessel motions by providing a buoyancy force as the bow pitches into a wave. As a consequence, the vessel does not have a traditional flat wet deck in the fore part of the vessel; rather, it has a centrebow with an archway wet deck on either side. The centrebow is 26 % of the overall length of the vessel, with the wet deck aft of the centrebow being flat.

Modifications were made to *HSV-2 Swift* to meet the specific requirements of the US Navy. She was fitted with a

Fig. 4 Bow view of HSV-2 Swift showing the centrebow between the demihulls

Table 1 Incat Hull 61 Main Parameters

Length overall	97.22 m
Length waterline	92.00 m
Beam overall	26.6 m
Draft fully loaded	3.436 m
Demihull beam	4.50 m
Deadweight	670 tonnes
Lightship displacement	1130 tonnes
Full displacement	1800 tonnes
Prime movers	4 × resiliently mounted Caterpillar 3618 marine diesel engines, each rated at 7200 kW at 100 % MCR
Waterjets	4 × Wartsilia LIPS LJ120E waterjets
Fuel (operating)	190,080 l
Fuel (long range)	2 × 210,238 l
Ride control system	Maritime dynamics active ride control system: active trim tabs aft and optional fold-down T-foil located at aft end of centre bow fitted with active fins
Speed	38 knots (operational)
	42 knots (lightship)
Class Society	Det Norske Veritas
Certification	DNV +1A1 R1 HSLC Cargo EO HELDK

stern ramp capable of on/off loading directly astern or to the starboard quarter, as well as a NAVAIR certified helicopter flight deck for operation of MH-60's, CH-46, UH-1 and AH-1 helicopters.

The main parameters of the vessel can be seen in Table 1. To increase passenger comfort and range of operability, the vessel is equipped with an active ride control system. This includes active trim tabs mounted at the transom and a retractable T-foil with active fins, mounted on the centreline plane at the aft end of the centrebow.

2.2 Measurements

The US Navy conducted full-scale trials with *HSV-2 Swift* (Hull 61) in coastal waters off Norway and off the northwest coast of the United Kingdom in the North Atlantic [11]. The aim of these trials was to acquire data for a range of wave environments and operating conditions, to allow assessment of the vessel's structural response, seakeeping performance and effectiveness of the ride control system.

The vessel underwent a series of octagons, each consisting of five legs starting with a head sea run and changing the course by 45° until following seas were reached. The vessel speed was kept constant throughout each octagon and the ride control T-foil configuration was also kept constant (either deployed or fully retracted); the trim tabs at the stern were always active. The length of each octagon leg varied with the relative wave heading to account for the varying encounter frequency; for head seas, the run time was 20 min; in beam seas, 30 min; and in following seas, it was extended to 40 min.

2.3 Monitoring system instrumentation and data acquisition

To determine the structural response, a total of 47 strain gauges were fitted at locations around the vessel. These strain gauges were split into three groups according to the type of structural response to be measured: global response (16 gauges), stress concentrations (21 gauges) and wave impacts (10 gauges).

Primary ship motions parameters, such as angles, rates and accelerations, were monitored at various locations around the vessel. The vessel roll and pitch was measured by using a gyrometer mounted at the LCG. To measure accelerations three axis accelerometers were mounted at the bow, bridge, LCG and flight deck. Several shipboard control systems were also monitored and recorded during the trials: position of T-foil and trim tabs, waterjet nozzle angle and waterjet shaft speed. Additionally, there were tie-ins to the ship's global positioning system (GPS) and gyro systems to allow the vessel's track, course and speed to be monitored.

The instantaneous absolute wave height was recorded using a Tsurumi Seiki Co. Ltd (TSK) radar-based wave-meter mounted on the bow. The wave direction was determined by visual observations of the ship's crew. Results from these observations are always approximated directions with a low directional resolution, normally 45°. Poor visibility due to the weather conditions or darkness can also reduce the accuracy of visual observations. Therefore, a method proposed by Davis et al. [12] was used to derive the ship's relative heading based on its heave, roll and pitch motions. The main wave direction is identified as the maximum angular slope of the ship, caused by pitch and roll motions. All data were recorded using an onboard data acquisition system logging at 100 Hz.

3 Slam identification

Strain signals at different locations in the fore part of the ship were examined to find an appropriate signal for slam identification and further analysis. Figure 5 shows some typical raw strain gauge traces recorded in the bow region of the vessel. With slamming defined as a rapid application of load on the vessel due to impact with the water, slamming can be seen in Fig. 5 as a rapid increase of stress in the structure. After impact, the vibratory response, also known as whipping, of the structure is also seen.

Since the slam impact is generally found to occur in the forward part of the ship, strain gauges in this area were chosen for further investigation. In this bow region, some strain gauges clearly showed slam events with a rapid increase of stress and the subsequent whipping behaviour. However, some strain gauges exhibited continuous whipping of the structure even without a slam having occurred; this made slam identification using these gauges impossible. The strain gauge identified for use in determining the occurrence and magnitude of slam events was strain gauge T2-18A, located in the centrebow archway and mounted on a stiffener cut out at frame 64; see Fig. 6 for a drawing of the location. In order to have consistency with regards to the magnitude of a slam event, a single strain gauge is required as a

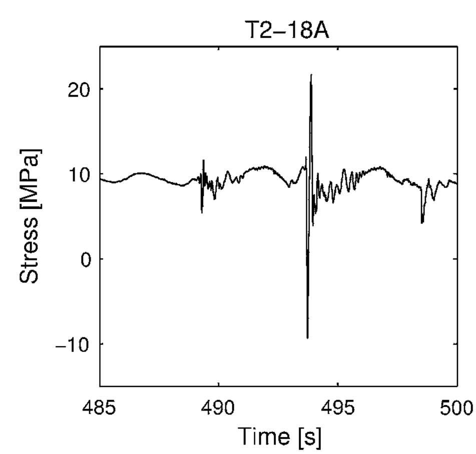

Fig. 5 Sample raw strain gauge data showing slam events at $T = 489$ and 494 s

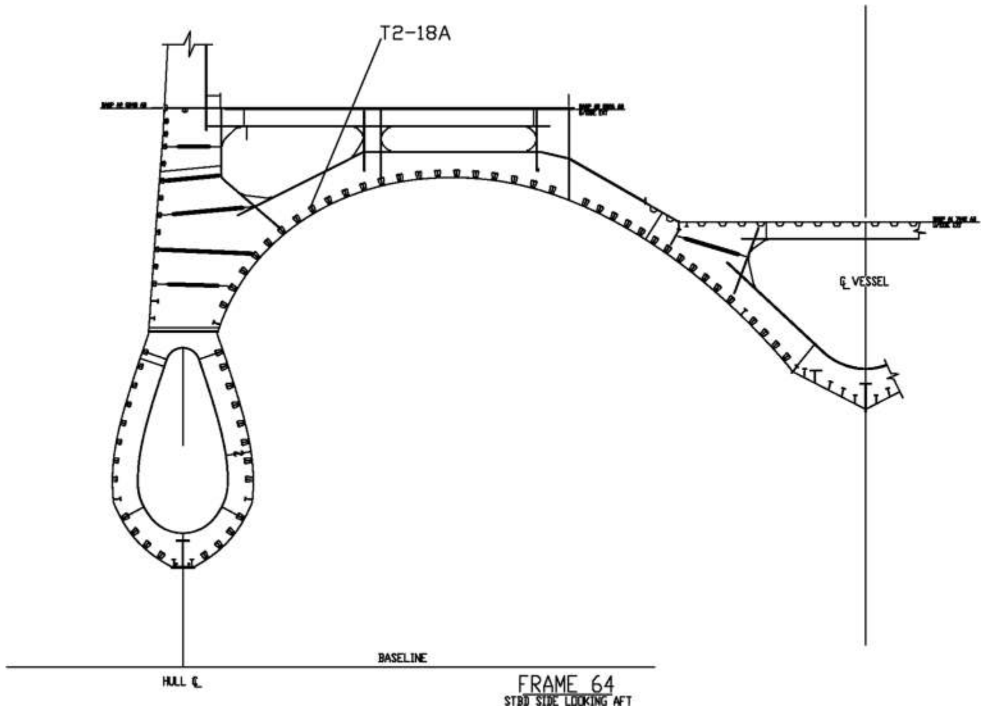

Fig. 6 Cross section of frame 64 showing location of strain gauge T2-18A

reference. Otherwise, some form of averaging would be required if multiple gauges are used to determine the slam magnitude. As for identification of the occurrence of slam events, analysis of the corresponding strain gauge on the other side of the vessel (T2-19A) showed that whilst some asymmetry can occur in the stress level resulting from the events, the slams were visible in both gauges.

In order for slam events to be identified in the data records, it was necessary first to define what constituted a slam event for this vessel. The strain gauge data was used to define a slam, since it ensures that only events that had an appreciable effect on the vessel structure were included in the definition. The practical difficulty of identifying slam events may be seen by examining Fig. 5. The slam occurring at $T = 494$ is clearly a slam event and would be easy to identify with a large number of different definition techniques. However, whilst it is proposed that the slam at $T = 489$ is also a slam event, due to its small peak, it may be difficult to classify it as a slam event using certain definitions. For example, a simple threshold method that identifies every peak exceeding a specified threshold value as a slam may misidentifying such slams, and also misidentify large global wave loads as slam events. Thomas et al. [8] used a rate of change of stress criterion, where a slam was identified if the rate of change exceeded the product of a specified rate constant with the yield stress of the material. Therefore, a slam was identified if a peak in the stress record occurred with:

$$\mathrm{d}\sigma/\mathrm{d}t > R_{\mathrm{c}} \cdot \sigma_{\mathrm{yield}}[\mathrm{MPa/\,sec}] \quad (1)$$

where $\mathrm{d}\sigma/\mathrm{d}t$ is the maximum rate of change of stress prior to the peak and R_c is the rate constant that has the units s^{-1}.

In the data records for *HSV-2 Swift*, the whipping after a slam event was also found to have a high rate of change of stress, which resulted in many whipping events being incorrectly identified in the records as slams.

Therefore, a second criterion was used in conjunction with the rate of change of stress criterion as follows.

The relationship between the ship motion and a slam event is shown in Fig. 7. The strain gauge signal is plotted versus the pitch signal and the ship relative velocity to the wave, with a negative pitch indicating a bow up motion. To make the structural response to slamming clearer, the strain gauge signal has been high-pass filtered with a cut-off frequency of 0.6 Hz. A cut-off frequency of 0.6 Hz was chosen since this is above the frequency of the global wave load, which had a maximum value of 0.297 Hz (35 knots in head seas). It is also significantly below the slam impact frequency and the ship natural frequencies ($\sim$2.6 Hz first longitudinal mode; $\sim$1.5 Hz lateral torsional mode). Prior to the slam, at $T = 412$ s, the relative vertical velocity reaches a maximum during a bow down motion. Then, due to the impact with the water surface, the vertical velocity decreases and the motion changes direction to a bow up motion. This relationship between downward bow motion and slam occurrence was used as a second criterion, with the assumption that only one slam occurred per downward

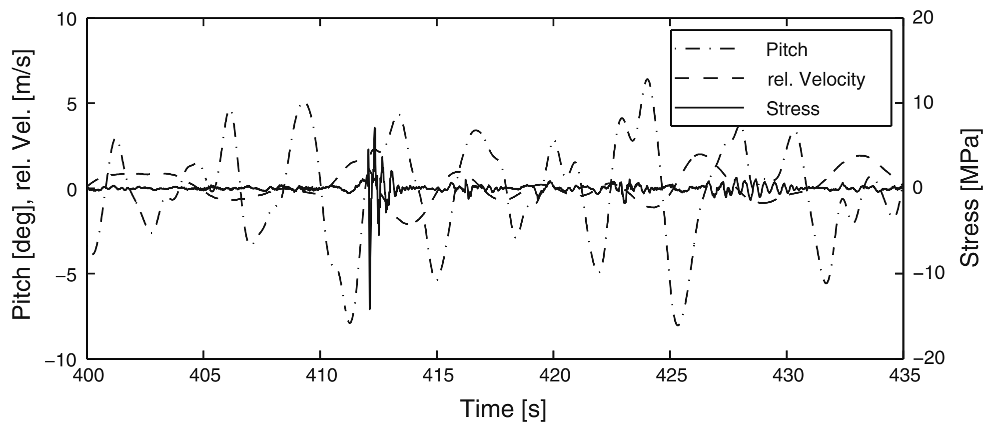

Fig. 7 Comparison of ship motions with filtered strain gauge data

bow motion. Thus, a combination of the rate of change of stress criterion and the downward bow motion, with not more than one slam per downward bow motion, ensured that the slam events were identified and the whipping events were excluded.

For the slam identification, an appropriate value for the rate constant was required. Firstly, the number of slams identified in the data records was determined as the value of rate constant was systematically altered. Figure 8 shows the rate constant versus the number of identified slams for different heading angles for strain gauge T2-18A. The rate constant of $R_c = 0.022$ can be seen to be a natural cut-off point in the curve, as the gradient changes markedly at this point. The number of slam events identified can be seen to increase rapidly as the slope criterion tends to zero, due to noise in the signal being incorrectly identified as slams. Secondly, the rates of change of stress of peaks, other than slam events, were investigated to ensure that the rate constant did not incorrectly identify them as slams. With the yield stress being 220 MPa, the rate of change prior to a peak, measured at strain gauge T2-18A, needed to exceed 5 MPa/s to be identified as a slam. This rate is the same as proposed by Thomas et al. [8] for Incat Hulls 042 and 050.

The boundary between a slam being defined as occurring and not occurring will always be nebulous. The approach presented is appropriate, particularly when it is borne in mind that changes to the rate constant affect the number of small, rather than large, slams being identified, since it is inclusive in defining stress peaks as slams. The authors propose that water impact events fall into three categories in decreasing order of stress magnitude: (a) large slams that can cause structural damage through a single event; (b) medium slams that have a major contribution to fatigue life reduction; and (c) small slams that have insufficient stress magnitude to contribute significantly to fatigue life reduction. This approach to slam definition has also been proposed by Dessi and Ciappi [13]. Fatigue analysis of this full-scale data has shown that generally, events with a magnitude of greater than 2 % of yield stress

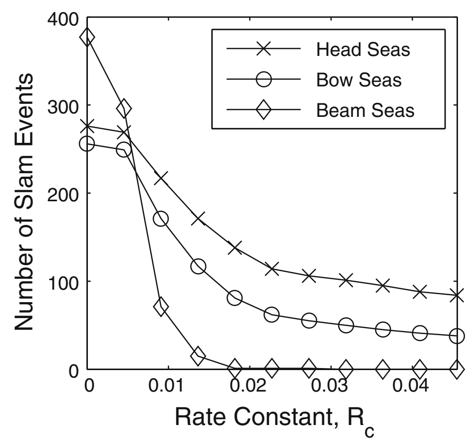

Fig. 8 Number of slam events versus rate constant

are required to make a significant contribution to a reduction of fatigue life. Therefore, it is clear that the method used to identify slam events here has identified slam events in all three categories.

The algorithm for slam detection, as outlined above, was programmed in Matlab to enable slams to be identified in all of the full-scale data records. The final check of the data was a visual examination to ensure that the algorithm had not neglected to identify any slam events.

Figure 9 illustrates the results of using this approach to identifying slam events, with five slams identified clearly in this sample of the data records. The raw data was high-pass filtered with a cut-off frequency of 0.6 Hz, to allow the maximum slam peak stresses to be determined without the influence of the global wave load.

4 Results and discussion

Using the previously described slam identification method, slam events were identified in the data records and analysed to determine their characteristics at different wave headings, vessel speeds, sea states and ride control system

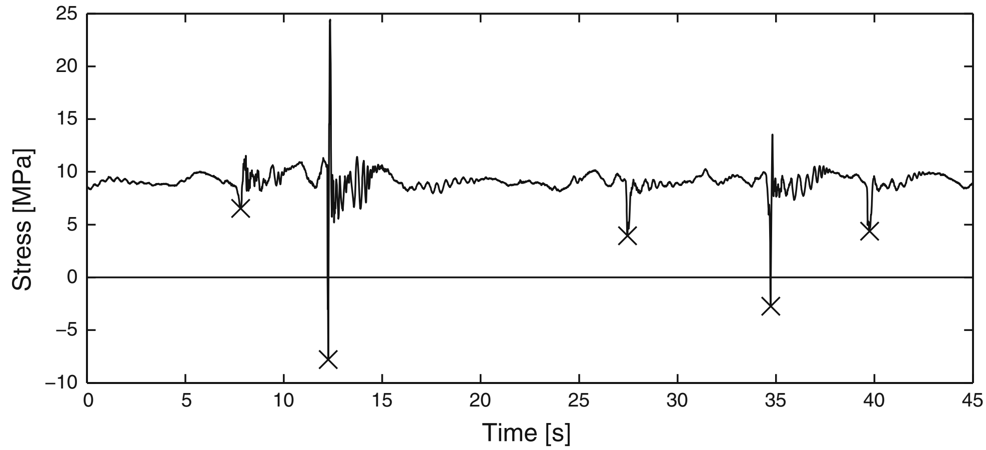

Fig. 9 Raw slam signal with identified slams marked with an X

Table 2 Trial conditions and overall slam occurrence rates

Octagon #	Run	Heading	$H_{1/3}$ (m)	T_0 (s)	Speed (knots)	RCS	Slams per hour	Measured slams
6	99	Head					523	169
	100	Bow	2.01	7.5	35	OFF	374	143
	101	Beam					234	127
12	145	Head					476	155
	146	Bow	1.62	7.3	35	ON	313	108
	147	Beam					94	47
13	152	Head					123	45
	153	Bow	1.38	7.5	30	OFF	109	24
	154	Beam					4	1
14	159	Head					339	114
	160	Bow	1.74	8.4	30	OFF	187	62
	161	Beam					2	1
19	192	Head					329	108
	193	Bow	1.90	7.6	30	ON	194	14
	194	Beam					27	14
21	206	Head					26	9
	207	Bow	1.60	7.2	15	OFF	4	1
	208	Beam					0	0

RCS ride control system

activation. Table 2 provides an overview of the conditions encountered during the analysed runs and the number of identified slams in each run. A statistical description of the slam occurrence rates and the severity of each slam was developed, helping to characterise slam events for different conditions.

Having determined the peak stress for every slam event, they were divided into bins based on their magnitude and plotted against their rate of occurrence. The magnitude of the slams were normalised by the yield stress of 220 MPa. Furthermore, the ship's motions, including maximum relative vertical velocity before each slam event, and the wave conditions were investigated relative to the severity of each slam.

To allow calculation of the significant wave height, the wave data needed to be converted from time domain to frequency domain using the discrete Fourier transform. The resulting energy density spectra were smoothed using Welch's modified periodogram method [14]. To reduce the variance in the spectrum, the time domain raw data was split into multiple segments and the smoothed spectrum was calculated as the average of the segments' spectra. To avoid spectral leakage, which is due to splitting the data into multiple segments, a window function was applied to every single segment. At a sample rate of 100 Hz, a Hanning window with a length of 8,000 samples provided good resolution. The overlapping of each window was 50 %, to prevent a loss of information due to the window function.

4.1 Influence of vessel speed

The influence of vessel speed on slam occurrence rates and maximum slam peak stresses is shown in Fig. 10 for head, bow and beam seas, comparing octagons 21 and 14, with the ride control system inactive. For all heading angles, severe slams are seen to occur rarely, while small slams have significantly higher occurrence rates. The distribution

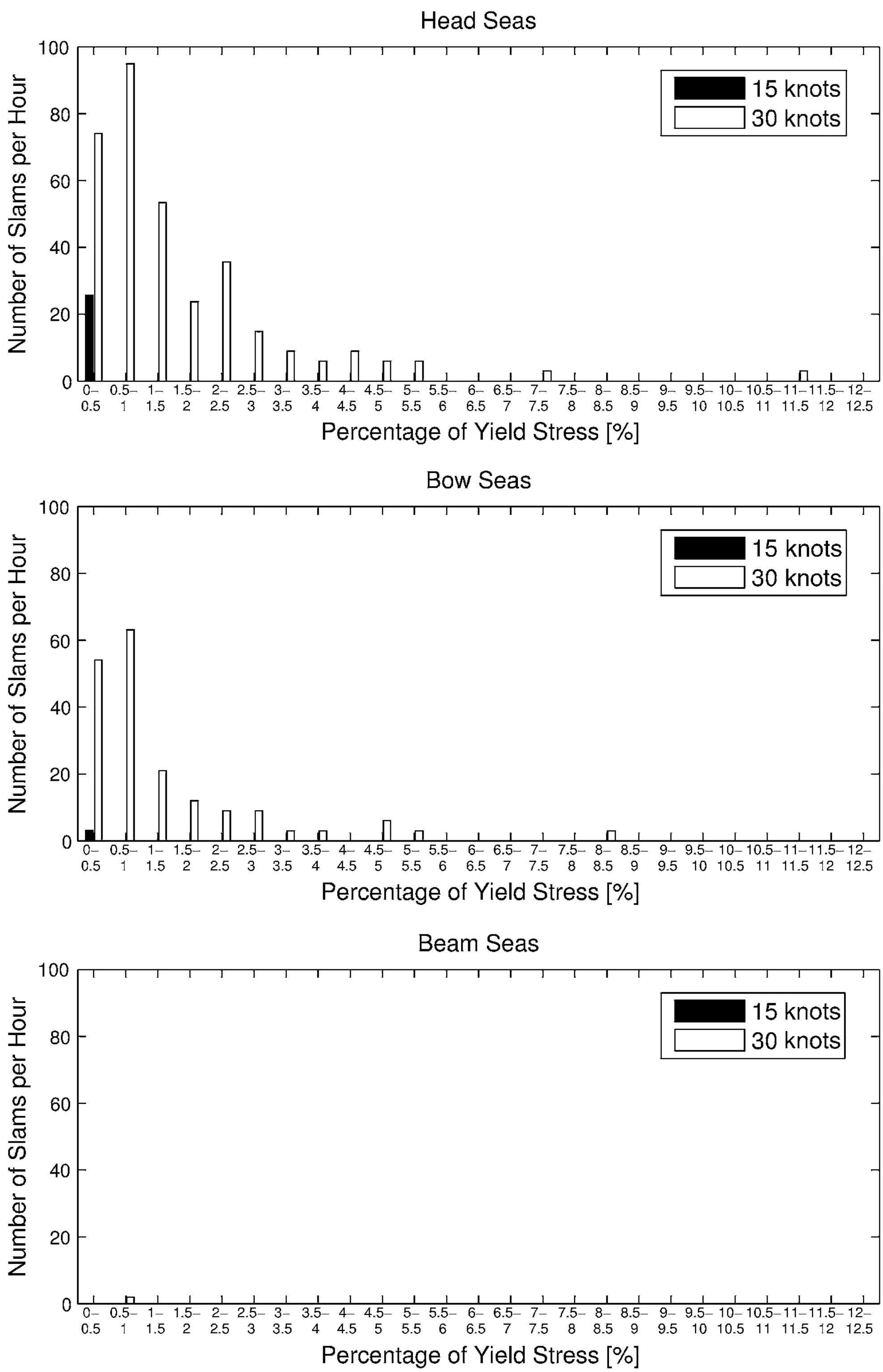

Fig. 10 Influence of speed on slam peak stress for varying wave headings (Octagons 14 and 21)

of slams along the x-axis shows that more than 50 % of the slams occur in a stress range of 0–1 % of yield stress. For larger slams, the occurrence rate rapidly decreases; for example, at a speed of 30 knots, only 8 slams per hour occurred above 5.5 % of yield stress.

A reduction of speed from 30 to 15 knots leads to a significant reduction in occurrence rates. In head seas, the total occurrence rate reduces from 339 slams per hour at 30 knots to only 26 slams per hour at 15 knots. The magnitude of the slams also reduces correspondingly: at 15 knots in head and bow seas there are no slams with a maximum normalised peak stress greater than 0.5 %, and no slam occurrence in beam seas. This shows that a reduction of speed minimises the possibility of severe slam occurrence that will directly influence the fatigue effect on the ship structure.

These results contrast with previous findings by Thomas [15], where for Incat Hull 050, a 96 m high-speed catamaran, a significant number of severe slams were measured in a slow speed condition. This difference may have been due to the larger sea state encountered by Hull 050. While the *HSV2-Swift* results are for encountered significant wave heights of 1.6–1.74 m; Hull 050 full-scale results were in significant wave heights of up to 7 m. Therefore, it is important to note that whilst reducing speed can lessen the occurrence and severity of slams, it does not necessarily prevent severe slams from occurring.

Comparing the different heading angles shows a clear decrease in the number of slams occurring and their severity as the vessel moves from head to beam seas for both speeds tested. At 30 knots, the slam occurrence rate reduces from 339 per hour in head seas to 2 per hour in beam seas, whilst at the reduced speed, the occurrence rate reduces from 26 per hour in head seas to zero per hour in beam seas. The severity of the slams also reduces as the heading changes from head seas around to beam seas. This implies that if the operational option is available to change vessel heading when in severe sea states, a wave heading away from head seas will not only reduce the occurrence of slamming, but also reduce the severity of the slams.

4.2 Influence of seastate

To analyse the influence of the sea state on slamming behaviour, the slamming occurrences for octagons 13 and 6, which had significant wave heights of $H_{1/3} = 1.38$ and 2.01 m respectively, were examined. Results for head to beam seas are presented in Fig. 11. As already seen in the analysis of speed influence, small slams dominate with more than 50 % of the slams occurring within a stress range from 0 to 0.1 % of yield stress. In these sea states, severe slams seldom occur with very low occurrence rates at above 5 % of yield stress.

A clear difference between the results for $H_{1/3} = 2.01$ and 1.38 m can be seen. In the lower sea state, fewer slams occur as well as the slams having smaller maximum peak stresses. This increase in slam occurrence with increasing wave height is an expected result, since the absolute motions of the vessel will increase with wave height. However, the increase in occurrence rate is greater than would be expected for an increase in significant wave height of only 0.63 m, with the rate of slamming more than doubling in head seas and tripling in bow seas.

The most severe slams occurred in the 2.01 m head sea run, with a maximum peak stress of 10.5–11 %; the most severe slams in 1.38 m seas were only at 6–6.5 %. The same relationship between the maximum slam peak stresses for the different sea states can be noticed for bow and beam seas, but with maximum stresses becoming smaller as the heading angle changes from head to beam seas.

For the lower sea state, the slam occurrence decreased from head to beam seas for all slam magnitudes. In contrast, for the 2.01 m significant wave height there was an increase in the slam occurrence rate of smaller slams as the vessel changed, heading from head to beam seas. This high rate of occurrence of low level slams in beam seas was probably due to large roll motions causing filling of the archway and resulting in small wave impacts; the motions results from these full-scale trials can be found in Jacobi et al. [16]. That there were no significant slam events in beam seas reinforces this proposal, as the relative vertical velocities were probably low.

The relative vertical velocity between the bow and the water surface before every slam event was therefore calculated to investigate the change in behaviour for different operating conditions. Figure 12 shows that the relative vertical velocity for a slam significantly reduces from head to beam seas. It is interesting to identify the maximum relative vertical velocity for each sea state and heading angle: in $H_{1/3} = 2.01$ m, it reduces from 13 m/s in head seas to 6.5 m/s in beam seas, whilst for $H_{1/3} = 1.38$ m the reduction is from 11 to 0.1 m/s.

The trends for all heading angles show that the average relative velocity tends to be higher in high sea states, but also shows that the highest velocities do not always lead to the highest slam stresses. For example in the head sea run at 2.01 m, the most severe slam impact with a stress of 10.5 % of yield stress was at 7 m/s, whilst the impact with the largest relative velocity only lead to a slam stress of 3.8 %. A similar phenomenon can be observed for bow and beam seas where the highest relative vertical velocity does not lead to the highest slam stresses. So whilst there appears to be an overall trend, with a weak association, that larger relative vertical velocities result in larger slam impacts, the association is so weak that it cannot be used as a primary indicator of slam occurrence and magnitude.

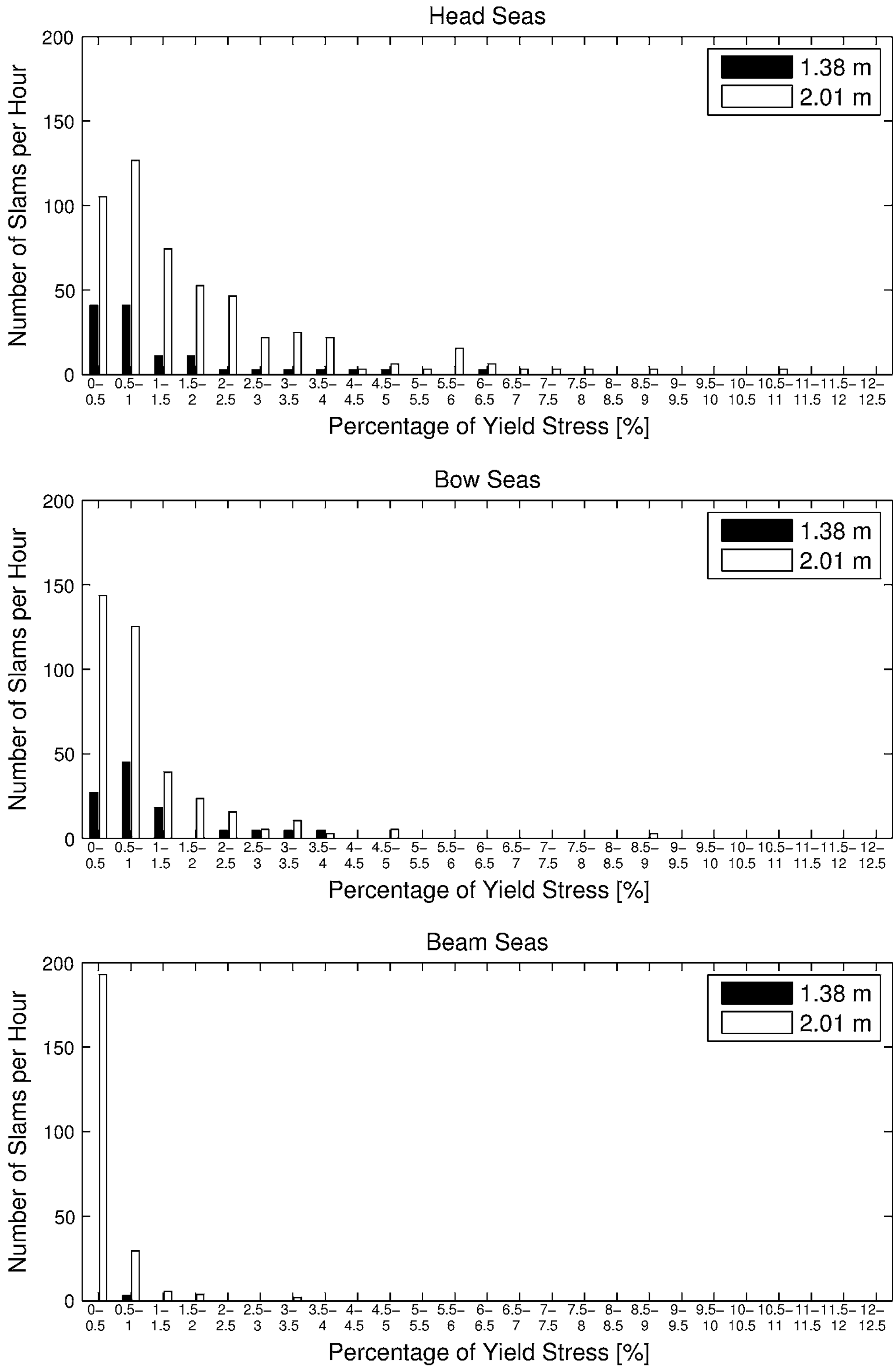

Fig. 11 Influence of sea state on slam peak stress for varying wave headings (Octagons 6 and 13)

This result is similar to that found in model test experiments [17] and shows that the traditional approach of Ochi and Motter [18] of using relative vertical velocity to predict slam occurrence and magnitude does not hold for large high speed catamarans. It is likely that there are other factors, as yet unknown, that are a stronger indicator of slam magnitude for such catamarans. For example, the manner in which the archway fills during a slam is likely to be critical and factors such as extent of filling, speed of filling and relative angle of water surface to vessel wetdeck

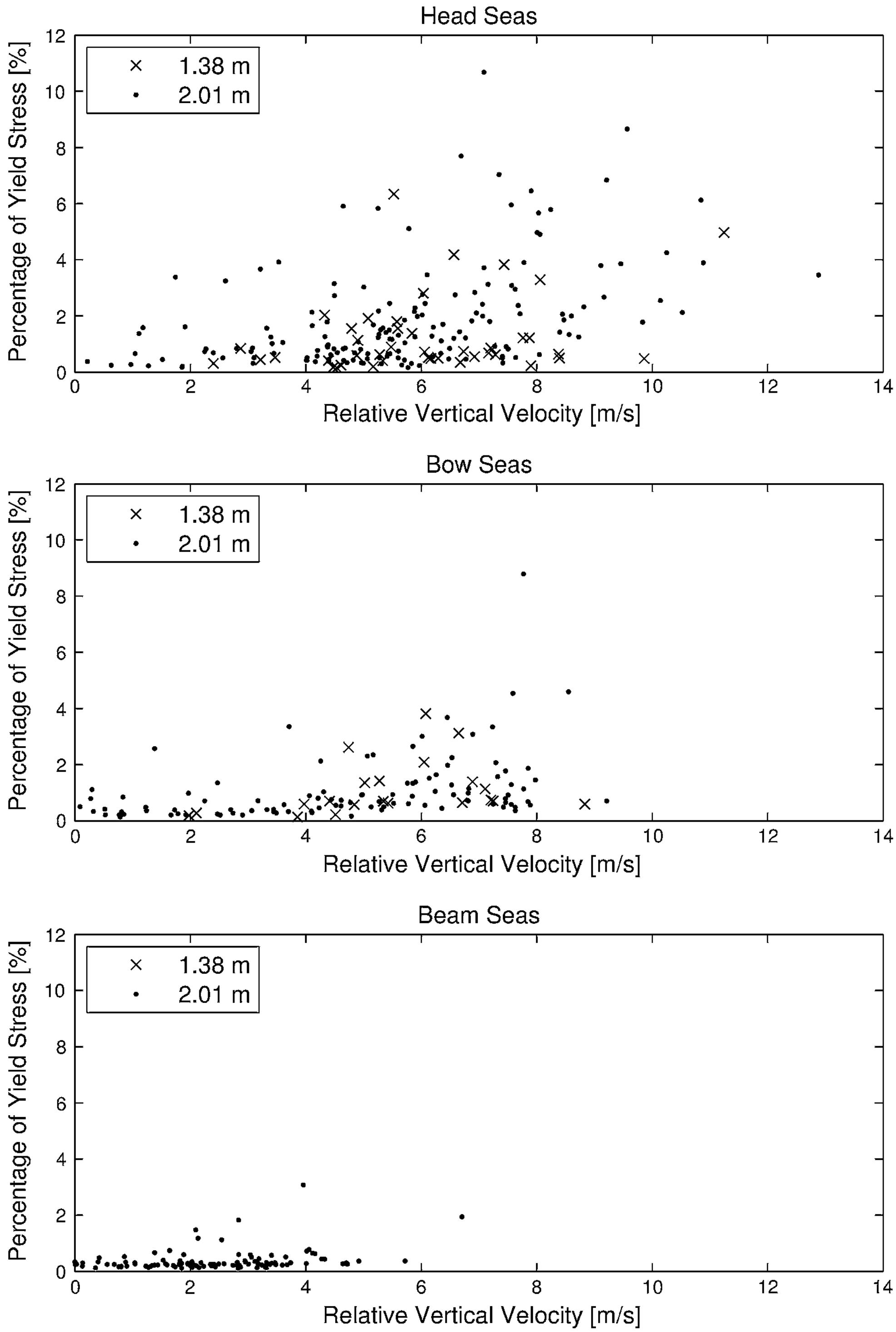

Fig. 12 Influence of sea state on maximum relative vertical velocity for varying wave headings (Octagons 6 and 13)

may have a considerable influence. Further work is required to try and clearly identify such effects and this work will likely involve further model testing where it is possible to install extensive instrumentation in the archway region to try and identify the key behavioural characteristics.

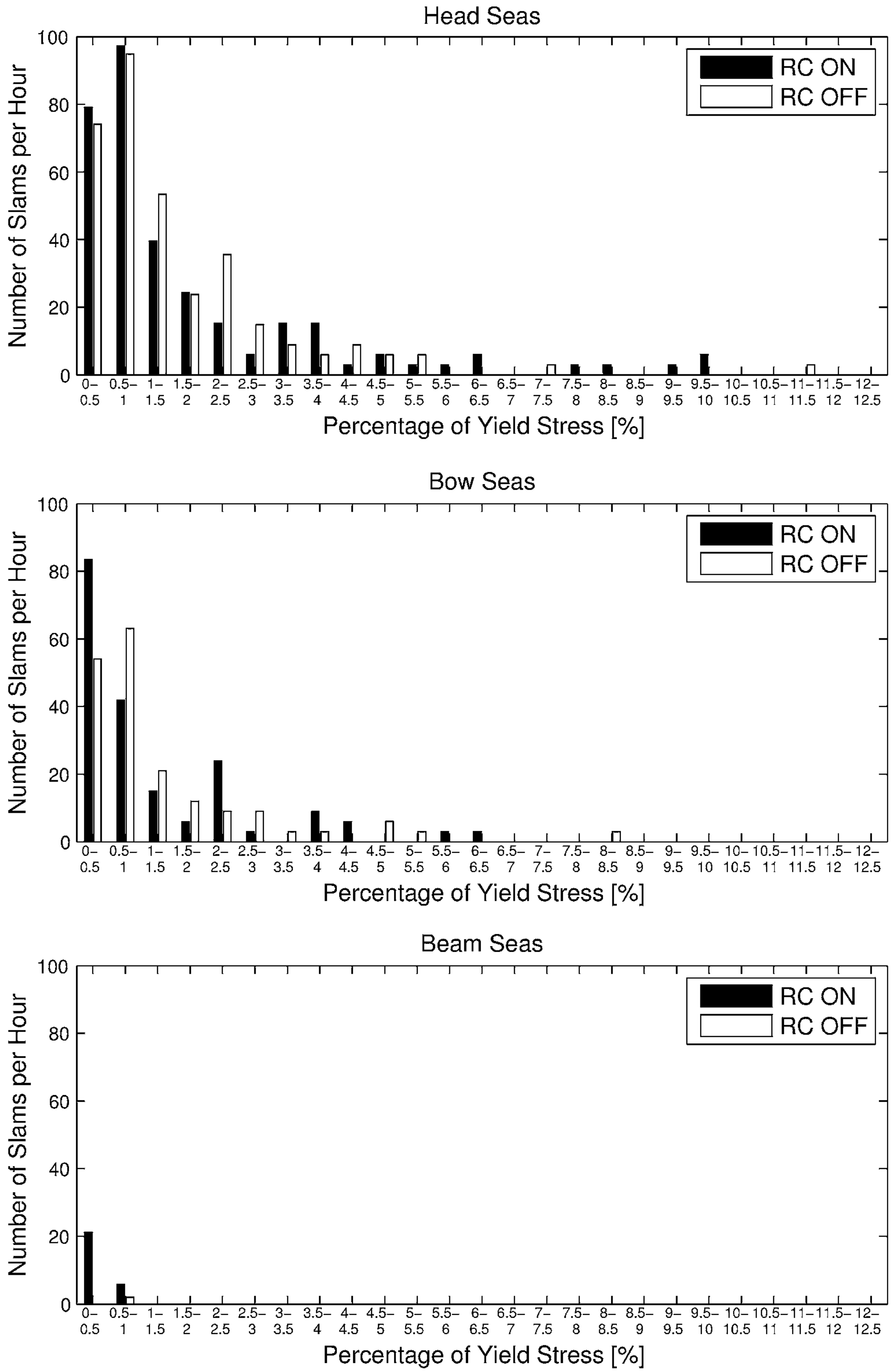

Fig. 13 Influence of ride control system on slam peak stress for varying wave headings at 30 knots (Octagons 14 and 19)

4.3 Influence of ride control system

As noted earlier, the *HSV-2 Swift* is equipped with an active ride control system (RCS) to increase passenger comfort and range of operability. The RCS has active trim tabs mounted at the transom of each demihull and a single retractable T-foil with active fins, mounted on the centreline plane at the aft end of the centrebow.

The change in slamming behaviour due to the RCS was monitored for vessel speeds of 30 knots and 35 knots. For 30 knots, the slam occurrence rates, measured during octagons 14 and 19, are plotted versus the

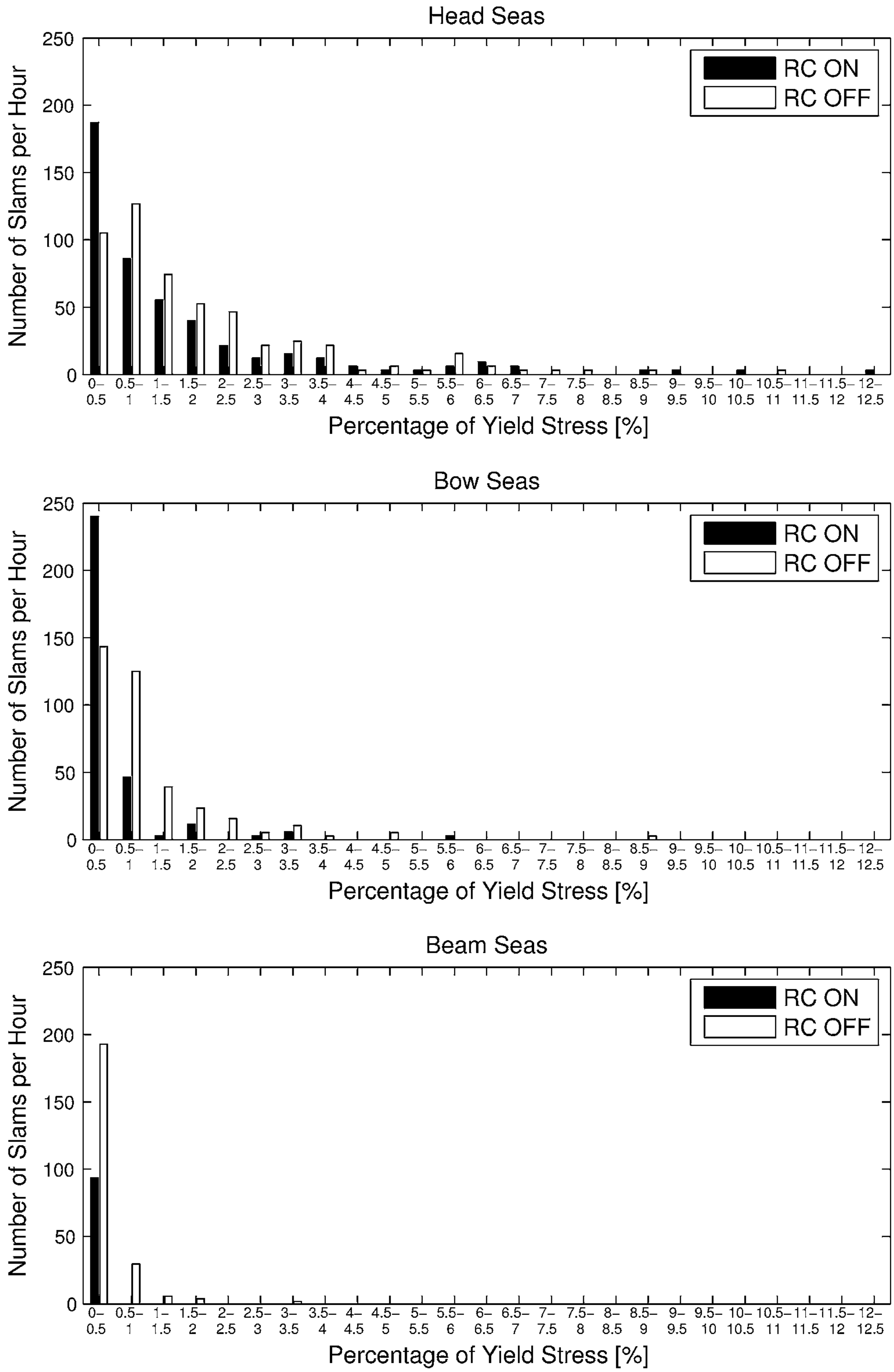

Fig. 14 Influence of ride control system on slam peak stress for varying wave headings at 35 knots (Octagons 6 and 12)

slam magnitude in Fig. 13 and the highest magnitude slam events were found in the runs with the T-foil deactivated. Note that the complete RCS was not deactivated, just the T-foil. In head seas, the maximum slam stress reduced from 11 to 11.5 % of yield stress with T-foil deactivated to 9.5–10 % with T-foil activated, and in bow seas the stress was reduced from 8–8.5 to 6–6.5 %.

Figure 13 shows that there are clear reductions of the overall occurrence rate when using the T-foil. However, looking at some single bins shows an increase of stress with the T-foil being activated. The reason for this may be

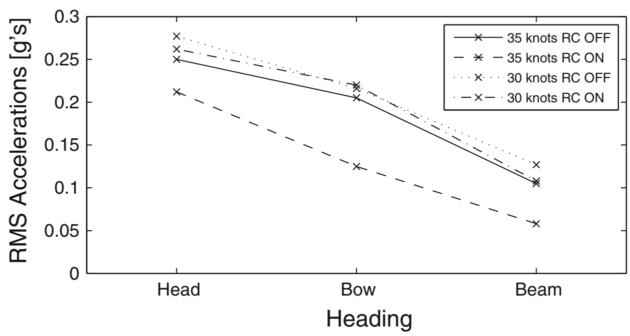

Fig. 15 *Vertical* Accelerations in the Bow Region

that whilst the motions of the vessel reduce when the ride control is activated at the speed of 30 knots, it is not a significant reduction. This was found when the motions of the *HSV-2 Swift* were analysed for different operating conditions, as reported in Jacobi et al. [16], and may be due to the RCS system being designed for operation a higher speeds, i.e. 35 knots and above, with lower forces resulting from the control surfaces at the slower speeds.

A clearer trend can be seen in the 35 knots runs of octagons 6 and 12. In Fig. 14, all heading angles show a reduction of slam occurrence rates with the T-foil being retracted; only for the very smallest slams can a higher occurrence rate be seen with the active T-foil for head and bow seas. Similarly to the 30 knots data, a reduction of the maximum slam peak stress can be seen in the bow and beam seas run. Interestingly, in the 35 knots head sea run with activated T-foil, the highest slam peak stresses in the analysed data were found to be at a stress of 12–12.5 % of yield stress.

Looking at the root mean square (RMS) values of the accelerations measured in the bow region of the vessel, which are presented in Fig. 15, clear motion reduction can be seen, especially for the 35 knots runs. This correlates with the trend observed in the slam occurrence rates. So, at high speed the RCS appears to be effective at reducing motions and slam occurrence, though it cannot prevent severe slams occurring.

The relative vertical velocities before each slam were also assessed for both conditions. Figure 16 presents the results for the various runs conducted at 30 knots, and Fig. 17 for 35 knots. Interestingly, for all headings, the highest velocities before a slam were measured in the activated T-foil condition. For head seas, a clear trend can be seen where high velocities also lead to high stresses. However, some of the highest velocities only lead to medium severity slam events, whilst medium relative velocities can lead to high slam magnitudes. Having seen a clear reduction of the motion, characterised by the RMS values of measured accelerations at the bow for the 35 knots run with active T-foil, no clear influence of the T-foil on the relative velocities prior to the slams can be seen. This result leads to the proposition that the actual slamming behaviour is independent of RCS system, and is dependent instead on the actual resulting motions and interaction between the water and the vessel hull.

In summary, the comparison of slamming behaviour with respect to RCS deployment demonstrates that the system has the best influence on motions and reduction of slam behaviour at the higher vessel speed, and at this speed can have a significant influence on the slamming behaviour. It is proposed that further work should be conducted on the influence of the RCS on vessel behaviour, since it may be possible that the control algorithm, which is currently focused on improving passenger comfort, may be able to be designed to reduce slam loads, and hence the global wave loads, experienced by the vessel.

5 Implications for vessel design and operations

The results clearly demonstrate that the vessel speed has a significant influence on slamming behaviour; for the conditions investigated reducing speed to 15 knots resulted in a low number of slam events and at low magnitudes when compared with operating at 30 knots. Operationally, this implies that major reductions in structural loadings can be achieved with speed reductions, and this should be taken into account when assessing the design load cases. Reducing speed will result in lower sagging moments on the demihulls and fewer stress cycles that can significantly influence the fatigue life of a large, welded aluminium vessel [5].

During the design process, identification of the likely wave environments for operation is critical. The strong influence of significant wave height on the occurrence and magnitude of slams, as seen in these results, demonstrates that the structural loading can increase dramatically with an increase in significant wave height. Therefore, to adequately ensure that the structural design is optimised, ensuring that sufficient strength is achieved whilst retaining a lightweight structure, the loading behaviour for the expected zone of operation should be identified.

The influence of the ride control system was found to be greater at the larger speed tested (35 knots). At this speed, it had a significant impact on reducing the vessel motions and slam occurrence rates, though large slams were still experienced by the vessel. This suggests that if hydrodynamic analysis is to be used during the design stages of a large high-speed catamaran to ascertain design loads, it should include the influence of a ride control system. However, the RCS cannot be expected, based on these results, to have a strong influence on

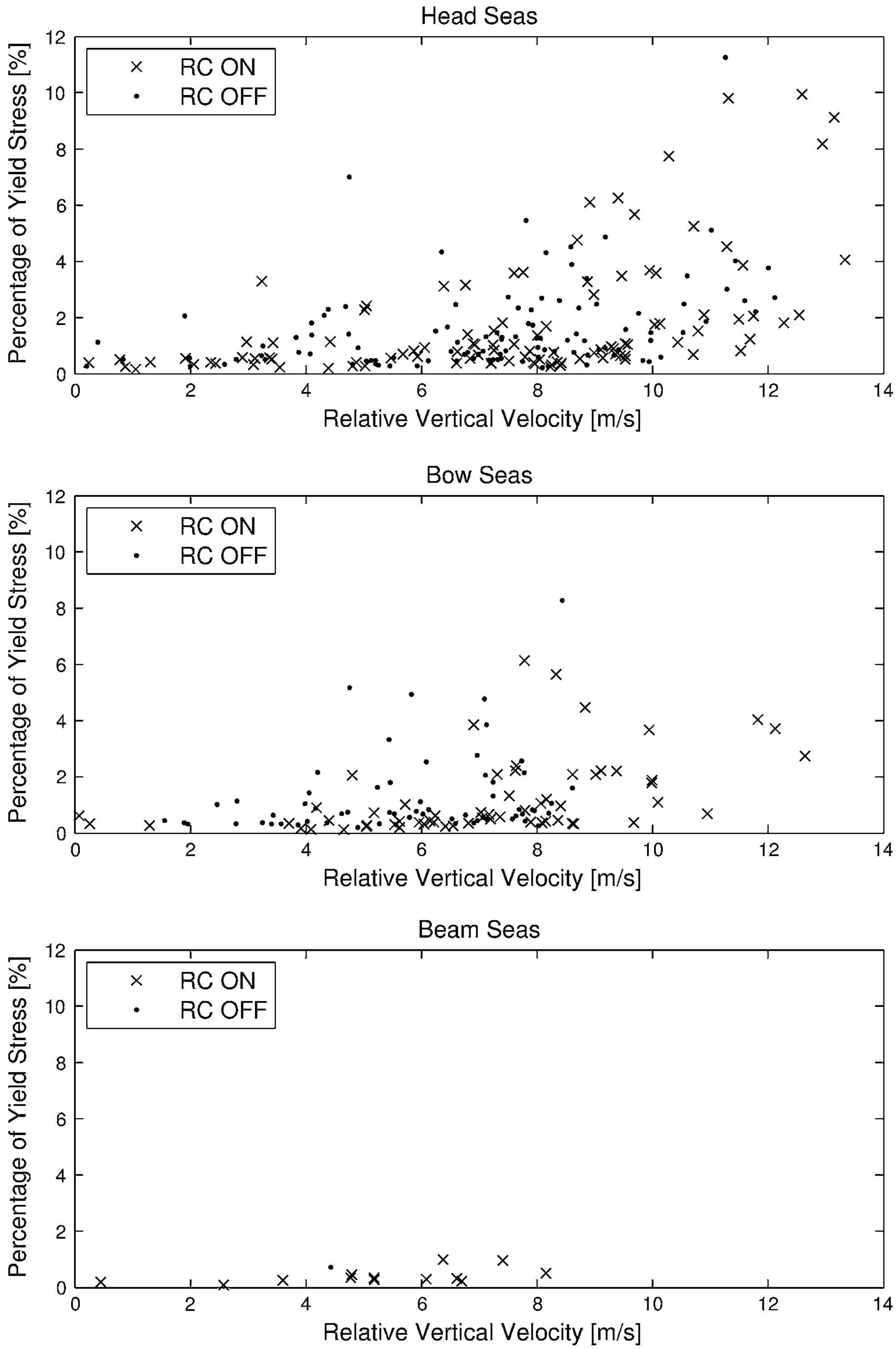

Fig. 16 Influence of ride control system on maximum relative vertical velocity for varying wave headings at 30 knots (Octagons 14 and 19)

structural loadings at speeds below the design operating speed. It is proposed that the control algorithm of the RCS should be investigated further, to determine if a different control strategy can result in greater reductions of slam occurrences and magnitudes.

Using a methodology proposed in Thomas et al. [3], it could now be possible to further analyse these slam events to ascertain the wave loadings for a series of different slam events using finite element analysis. This would result in knowing the bending moments for the slam events to

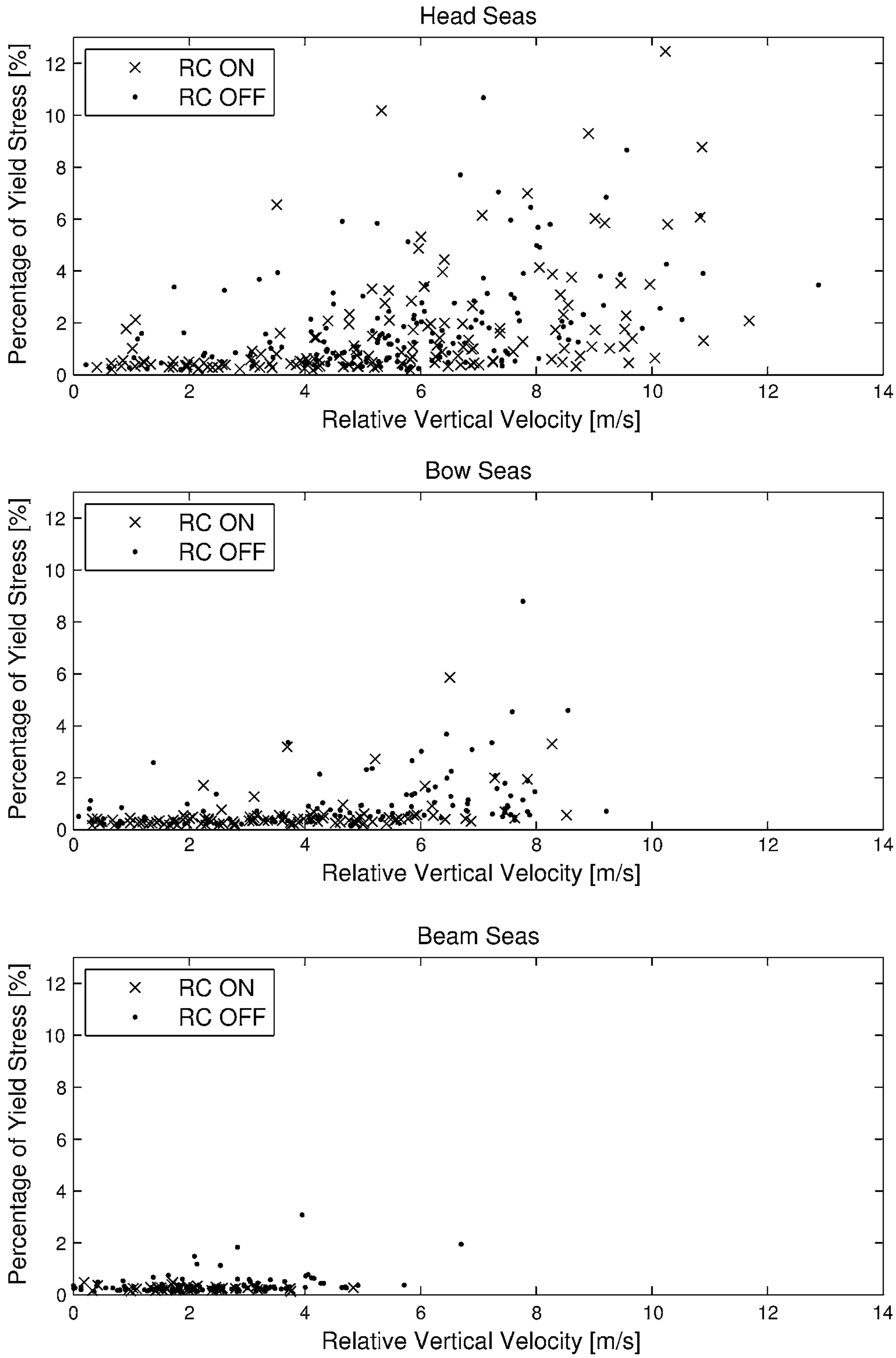

Fig. 17 Influence of ride control system on maximum relative vertical velocity for varying wave headings at 35 knots (Octagons 6 and 12)

reconcile them against the design load cases defined by Classification Societies. Additionally, the influence of the slamming and subsequent whipping behaviour on fatigue life could be determined for different components of the structure.

6 Conclusions

Data from full-scale trials completed on *HSV-2 Swift*, a 98 m Incat catamaran while operating in coastal waters off Norway and off the north-west coast of the United

Kingdom in the North Atlantic have been analysed for varying wave headings, vessel speeds and sea states. A series of slam events was identified in the data records using an automatic slam identification algorithm, considering the measured rate of change of stress in the ship structure coupled with the vessel's pitch motion.

This database of slam events allowed slam occurrence rates to be found for a range of conditions and the influence of vessel speed, wave environment and heading to be determined. The slam events were further characterised by assessing the relative vertical velocity at impact between the vessel and the wave. The influence of a ride control system on the slam occurrence rates has also been assessed.

The influence of vessel speed on slam occurrence rates and maximum slam peak stresses was found to be significant, with a reduction of speed from 30 to 15 knots leading to a large reduction in occurrence rates. The magnitude of the slams also reduced correspondingly; at 15 knots in head and bow seas, there were no slams with a maximum normalised peak stress greater than 0.5 % of yield stress, and no slam occurrence in beam seas. This shows that a reduction of speed minimises the possibility of severe slam occurrence, which will directly influence the effect on the ship structure.

Comparing the different heading angles, there was a clear decrease in the number of slams occurring and their severity as the vessel moves from head to beam seas for both speeds tested. The severity of the slams also reduced as the heading changed from head seas around to beam seas. This suggests that if the operational option is available to change vessel heading when in severe sea states, a wave heading away from head seas will not only reduce the occurrence of slamming, but also reduce the severity of the slams.

By investigating the influence of sea state on slamming behaviour, it was clear that in the lower sea state, fewer slams occur, as well as the slams having smaller maximum peak stresses, since the absolute motions of the vessel will increase with wave height. The relative vertical velocities between the ship and the wave showed that whilst there appears to be an overall trend, with a weak association, larger relative vertical velocities result in larger slam impacts. However, the association is so weak that it cannot be used as a primary indicator of slam occurrence and magnitude.

The influence of the ride control system was found to be greater at the larger speed tested (35 knots). At this speed, it had a significant impact on reducing the vessel motions and slam occurrence rates, though large slams were still experienced by the vessel. This suggests that if hydrodynamic analysis is to be used during the design stages of a large high-speed catamaran to ascertain design loads, it should include the influence of a ride control system. However, the RCS cannot be expected, based on these results, to have a strong influence on structural loadings at speeds below the design operating speed. It is proposed that the control algorithm of the RCS should be investigated further, to determine if a different control strategy can result in greater reductions of slam occurrences and magnitudes.

Acknowledgments The authors acknowledge the work of Naval Surface Warfare Center, Carderock Division, USA in conducting the full-scale measurements, and thank them for making the data available for analysis.

References

1. Blunden A (ed) (1990–2011) Fast ferry international. Fast Ferry Information Ltd, London, UK
2. Rothe F, Sames P, Schellin T (2001) Catamaran wetdeck structural response to wave impact. In: Proceedings of the 6th international conference on fast sea transportation (FAST2001) 3. Southampton, UK, pp 125–133
3. Thomas G, Davis MR, Holloway DS, Roberts T (2003) Transient slam response of large high speed catamarans. In: Proceedings of the 7th international conference on fast sea transportation (FAST2003) 2. Ischia, Italy, pp B1.1–B1.8
4. Thomas G, Davis MR, Holloway DS, Roberts T (2008) The vibratory damping of large high-speed catamarans. Marine Struct 21(1):1–21
5. Thomas G, Davis MR, Holloway D, Roberts T (2006) The influence of slamming and whipping on the fatigue life of a high-speed catamaran. Aust J Mech Eng 3(2):165–174
6. Steinmann P, Fach K, Menon B (1999) Global and slamming sea loads acting on an 86 m high speed catamaran ferry. In: Proceedings of the 5th international conference on fast sea transportation (FAST1999). Seattle, USA, pp 709–718
7. Roberts T, Watson N, Davis MR (1997) Evaluation of sea loads in high speed catamarans. In: Proceedings of the 5th international conference on fast sea transportation (FAST1997). Sydney, Australia, pp 311–316
8. Thomas G, Davis MR, Holloway DS, Watson N, Roberts T (2003) Slamming response of a large high-speed wave-piercer catamaran. SNAME Marine Tech J 40(2):126–140
9. Amin W, Davis MR, Thomas G, Holloway DS (2009) Slamming quasi-static analysis of an incat 98-m high-speed wave piercing catamaran. In: Proceedings of the international conference for innovation in high speed marine vehicles, Fremantle, Australia
10. Fu TC, Fullerton AM, Terrill E, Faller W, Lada G, Hess D, Minnick L (2009) Measurement and modeling of the motions of a high-speed catamaran in waves. In: Proceedings of the 28th international conference on ocean, offshore and arctic engineering (OMAE2009), Honolulu, Hawaii, USA
11. Brady TF, Bachman RJ, Donnelly MJ, Griggs DB (2004) *HSV-2 Swift* instrumentation and technical trials plan. Technical Report, Naval Surface Warfare Center Carderock Division
12. Davis MR, Watson N, Holloway DS (2005) Measurements of response amplitude operators for an 86 m high-speed catamaran. J Ship Res 49(2):121–143
13. Dessi D, Ciappi E (2013) Slamming clustering on fast ships: from impact dynamics to global response analysis. Ocean Eng 62:110–122
14. Welch PD (1967) The use of fast fourier transform for the estimation of power spectra: a method based on time averaging over short, modified periodograms. IEEE Trans Audio Electroacoust 15:70–73
15. Thomas G (2003) Wave slam response of large high speed catamarans. PhD Thesis, University of Tasmania

16. Jacobi G, Thomas G, Davis MR, Holloway DS, Davidson G, Roberts T (2012) Full-scale motions of a large high speed catamaran: the influence of wave environment, speed and ride control system. Int J Maritime Eng (RINA Trans Part A) 154(A3): 143–155
17. Thomas G, Winkler S, Davis M, Holloway D, Matsubara S, Lavroff J, French B (2011) Slam events of high-speed catamarans in irregular waves. J Mar Sci Technol 16(1):8–21
18. Ochi MK, Motter LE (1973) Prediction of slamming characteristics and hull responses for ship design. Trans SNAME 81:144–176